# THE EFFECTS OF ELMS ON THE PLASMA EDGE OF JET

**J Lingertat,** B Alper, S Ali-Arshad, P E Bak[1], A Chankin, S Clement, P Coad, I Cortes[2], N Deliyanakis, J Ehrenber, A Loarte, R Monk[3], L Porte, R Prentice and A Tabasso[1]

JET Joint Undertaking, Abingdon, Oxfordshire, OX14 3EA, UK
[1] Imperial College, Plasma Physics Depart., Prince Consort Road, London, SW7 2BZ, UK.
[2] Asociacion Euratom/Ciemat, 28040 Madrid, Spain.
[3] Royal Holloway College, University of London, Surrey, TW20 0EX, UK.

**INTRODUCTION** - ELMs are an unavoidable ingredient of H - mode plasmas in tokamaks. They are associated with a pulse-like release of energy and particles from the main plasma into the divertor. This may adversely affect the divertor operation or in the case of high power operation, even damage the divertor target plates. On the other hand, it is well known that ELMs are beneficial in reducing the density and impurity build-up in H-mode discharges. To exploit these beneficial features of the ELMs and to avoid the detrimental ones a thorough understanding of their generation and of then energy release mechanism is necessary. This paper focuses on the details of the ELM - triggered energy and particle release into the divertor.

For analysis, mostly giant ELMs (Type I) have been used which are observed after the ELM-free phase of high performance NB-heated discharges [1].

**SUMMARY OF RECENT JET RESULTS** - During an ELM the release of energy and particles from the main plasma into the divertor occurs in a sequence of three phases:

- Phase I the "precursor" phase with a characteristic time of $\delta t_p \leq 100\ \mu s$
- Phase II the "plasma edge determined" phase with a characteristic time $\delta t_e \sim 100\ \mu s$,
- Phase III the "confinement degradation" phase with a characteristic time $\delta t_c \sim 10 - 50$ ms.

*Phase I* - The precursor phase is observed at the divertor as a perturbation of the floating potential measured by the target Langmuir probes. Since the floating potential is mainly determined by the electron temperature and the current flow between plasma and target, this phase may be regarded as the beginning of the increase of the power flux into the divertor caused by electron heat conduction. The total amount of deposited energy on the divertor target plates is below the detection limit ( $\sim 10^4$ J).

During an ELM the perturbation of the floating voltage starts usually $\delta t_p \sim 10 - 100\ \mu s$ earlier than the density increase measured by a divertor interferometer. This feature is not observed with every ELM. Often the floating voltage precursor is correlated with precursors observed by the reflectometer and by magnetic probes.

A comparison between the time of arrival of the floating voltage perturbation on the outer and inner strike zones shows no time difference to within 20 μs. However, there is a time difference of 0.5 - 1 ms between the signals obtained by a reciprocating probe inserted near the top of the plasma and the target probes [2]. This implies that the X-point region is the origin of the perturbation [2,3,4].

*Phase II* - During the plasma edge determined phase, up to a few percent of the main plasma stored energy is released within $\delta t_e \sim 100\ \mu s$ into the divertor. This energy is removed from the outer region of the plasma column [5] and assumed to be transported mainly by electron heat conduction. A similar model has been proposed for type III ELMs [6].The maximum parallel power flux may reach values of $\sim 10^4\ MW/m^2$. A transient connection between the target surface and a plasma of ~ 300 - 400 eV gives the right order of magnitude for the measured power flux.

The soft X-ray intensity perturbation caused by an ELM is shown in fig. 1. Here, the perturbation starts at the top of the plasma, moves down to the X-point and again up to the top. Note, however, that other ELMs have been observed which start near the X-point region. There is no evidence of the outer midplane being the origin of ELMs [7]. The fastest time scale found in this data is $\sim 10\ \mu s$ which may be associated with the precursor time scale $\delta t_p$. The total time of the perturbation is $\sim 100\ \mu s$. This time interval is associated with the phase II time scale $\delta t_e$.

From the time evolution of the floating voltage and the surface temperature (figs.2 and 3) it is evident that during this phase the strike points of the separatrix move rapidly ($< 100\ \mu s$) inwards (inner strike point) and outwards (outer strike point) by $\Delta R_S \sim 20$ cm. The energy deposition has its maximum at the new position of the inner strike point. For the inner strike point $\Delta R_S$ may be so large that the main energy is released outside the divertor target onto structures of the inner wall.

Assuming that the plasma column behaves like a rigid body the observed movement of the strike points translates into a movement of the main plasma upwards and inwards with $\Delta z \sim 10 - 20$ cm and $\Delta R_p \sim 5 - 10$ cm. The observation of multiple peaked and broadened profiles on the divertor target reported previously [2] is caused by poor time resolution of the diagnostic instruments.

The high power flux pulse causes a release of impurities and deuterium from the affected areas which leads to the $D_\alpha$ - intensity peak usually associated with an ELM, to a peak in the radiated power and to an increase of the plasma density. The amount of released material and gas depends on the history of the surface hit by the power flux pulse. However, it is generally large because the target areas involved are regions with loosely bound deposition layers of non - stochiometric mixtures of impurities and gas.

Finally, the impurity/deuterium release triggers a deterioration of the global plasma energy confinement.

*Phase III* - During the confinement degradation phase the plasma loses particles and energy due to a drop in the relevant confinement times. This drop shows in most cases the features of an H → L transition [8].

The loss of particles leads to a decrease in the total particle content of the main plasma. The time evolution of the averaged density depends on the balance between the increase due to the injected impurities and deuterium during phase II and the subsequent decrease in the particle confinement time.

The loss of energy leads to an enhanced power flux to the target plates in a time scale of several 10 ms. This energy is deposited at the initial position of the strike points with an asymmetry of the power flux commonly observed during H → L transitions. The

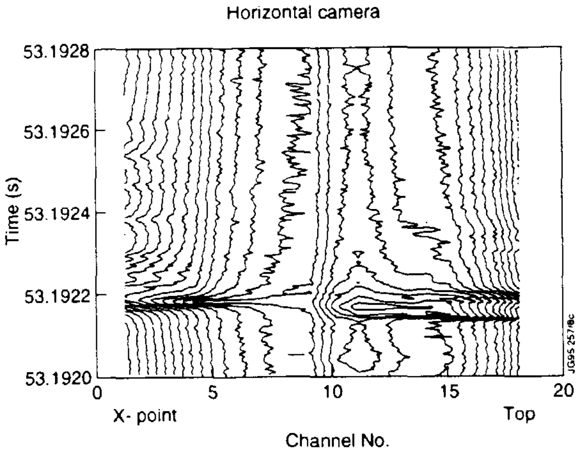

*Fig. 1 Contour plot of the soft X-ray intensity as a function of time measured by a horizontal camera with 18 lines of sight, pulse 33701*

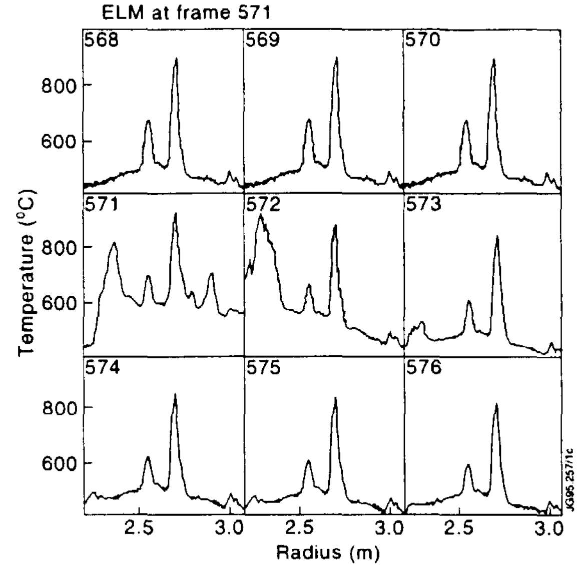

*Fig.2 Evolution of the target temperature profile before, during and after an ELM, pulse 33649.*

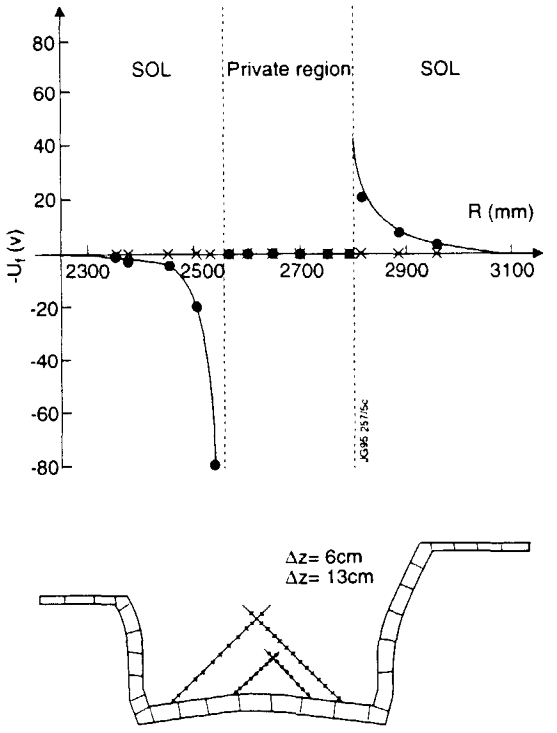

*Fig.3 Reconstruction of the movement of the X-point from the measured movement of the strike points together with the floating voltage distribution on the target plate before and during an ELM, pulse 33649*

total amount of energy lost during phase III depends on the extent of confinement degradation and is usually by a factor 2 - 8 larger than the energy loss during phase II (fig.4). After the H → L transition the plasma recovers within several 10 ms and goes again into the H mode. However, depending on the amount of injected impurities during phase II, the plasma may show a reduced H factor or even, after a sequence of giant ELMs, remain in the L mode.

The neutral gas pressure below the divertor target plate measured by pressure gauges [9,10] shows a spike for each ELM. Additionally, there is a "pile-up" of the base line pressure in the case of switched off cryo-pump. The $D_\alpha$ intensity shows the same pile-up behaviour, whereas the ion saturation current does not show this feature. The pile up is caused by neutral gas not taking part in the recycling process which indicates that there is a strong neutral gas source at the target caused by the ELMs. This additional gas can be removed by operating the cryo pump which is located below the target in the region of the outer strike point. With the cryo pump switched on the ELM frequency is reduced. Presumably, the neutral influx near the X-point region influences the ELM generation mechanism.

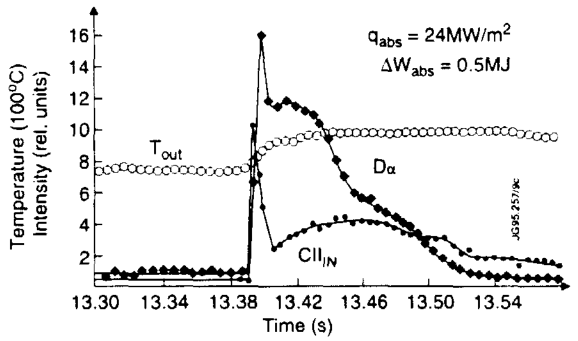

*Fig.4 Time evolution of the maximum target temperature at the outer strike point $T_{out}$, the average of the maximum $D_\alpha$ intensity at the inner and outer strike point $D_\alpha$ and the maximum of the CII radiation intensity at the inner strike point $CII_{IN}$ during an ELM, pulse 34458.*

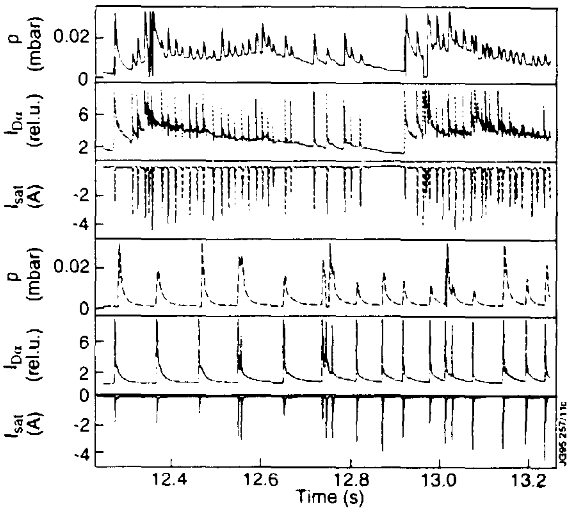

*Fig.5 Time traces of the neutral gas pressure p beneath the outer target plate, the $D_\alpha$ intensity and the ion saturation current during two ELMy discharges with cryo pump off (pulse 32270) and cryo pump on (pulse 32285).*

**Acknowledgement** - The support of Task Force H and the continuous help of P.Van-Belle with data processing is gratefully acknowledged.

## References

1 T.T.C. Jones et al., "The Route to High Performance on JET", this conference.
2 J. Lingertat et al., "The Effect of ELMs on the JET Divertor Plasma", Proceedings of the IPP/JET/Culham Workshop on H-mode and Boundary/Divertor Physics, JET 7 - 8 Nov. 1994.
3 O. Pogutse et al., "Edge Modes as ELM Events", this conference.
4 M.F.F. Nave et al., Nucl. Fusion 35(1995)409.
5 T.C. Hender et al., "Influence of Edge Instabilities on JET High Performance", this conference.
6 H. Zohm et al., 20th EPS Conf. on Contr. Fusion and Plasmaphys., Europhysics Conf. Abstracts 17C, 19.
7 D.N. Hill et al., Nucl. Fusion 28 (1988) 902.
8 V.V. Parail et al., "The Physics of L and H mode confinement in JET", submitted to Nucl. Fusion.
9 J.K.Ehrenberg et al. "Neutral Gas Pressure Measurements in the JET Pumped Divertor", this conf.
10 G. R. Saibene et al., "Effects of active pumping and fuelling on divertor plasma discharges in JET", this conference.